Contrib Mineral Petrol (2003) 145: 481–491
DOI 10.1007/s00410-003-0463-0

ORIGINAL PAPER

Rolf L. Romer

Alpha-recoil in U–Pb geochronology: effective sample size matters

Received: 9 December 2002 / Accepted: 26 February 2003 / Published online: 24 April 2003

Abstract Displacement of the daughter isotope by α-recoil results in an open system on the nanoscale. For a heterogeneous distribution of U and Th, this redistribution of intermediate and stable daughter isotopes results in subvolumes with a deficit of Pb and others with an excess of Pb. Whether such heterogeneities affect the analyzed U–Pb system depends on: (1) the volume of the analyzed sample, (2) the degree and scale of heterogeneity in the U and Th distribution, and (3) the analytical procedure. Spatial separation of parent and daughter through α-recoil affects the U–Pb systematics of leached samples, where leaching gives access to domains less than 1 μm wide. Anomalous data patterns originating from recoil induced parent-to-daughter fractionation are more important if there are strong heterogeneities in the U and Th distribution, whereby Pb excess appears more pronounced than Pb deficit. Fractionation of parent and daughter elements through selective dissolution of U-REE-rich growth zones in zircon and U-inclusions in columbite, as well as the presence of U–Th-rich micro-inclusions in silicates dated using a step-leaching scheme, may result in anomalous $^{207}Pb_{rad}/^{206}Pb_{rad}$, scattered $^{206}Pb_{rad}/^{238}U$ and $^{207}Pb_{rad}/^{235}U$, and reverse discordance. The accumulated structural damage controls the leaching and dissolution behavior, but may also influence the non-stoichiometric element mobilization during sputtering or ablation in the analysis of U-rich samples by SHRIMP and LA-MC-ICP-MS.

Introduction

Basic requirements for U–Pb dating of minerals include: (1) the decay of ^{238}U and ^{235}U (and their intermediate daughter isotopes) is statistical and the rates of decay are constant; (2) the initial condition of the system is known, can be determined independently, or can be estimated sufficiently well; and (3) the analyzed material is representative for the sample. The statistical nature of the decay is obtained by considering a large number of decays, whereas the representative nature of the investigated material originally was thought to be secured by using a large number of crystals. Although the combination of the ^{235}U-^{207}Pb and ^{238}U-^{206}Pb decay schemes in the concordia diagram provides for the possibility of recognizing disturbances such as inheritance or loss of U and Pb, the superposition of several of these processes may introduce ambiguities into the interpretation of the geochronological significance of the data. Hence, undisturbed, single-stage crystals yielding concordant data are the most suited ones for most dating purposes. Undisturbed, single-stage crystals, however, often enough are not the only kind of crystal present in large (multi-grain) samples. Therefore, methods have evolved over the last decades towards higher selectivity in the choice of the dated mineral, more advanced sample preparation (magnetic separation, air-abrasion, leaching, step-wise dissolution), lower laboratory blanks (permitting smaller samples to be analyzed), and new instruments (SHRIMP, LA-MC-ICP-MS) with the goal to analyze smaller, yet better characterized samples (e.g., Krogh 1973, 1982a, 1982b; Compston et al. 1984; Parrish 1987; Steiger et al. 1993; Mattinson 1994; Sergeev et al. 1995, 1997; White et al. 2001). Reduction of sample size to individual crystals or parts of crystals raises the question to which extent the investigated crystals are representative for the studied process and to which extent the age determination on micro-samples is influenced by processes that operate on the nanoscale.

R. L. Romer
GeoForschungsZentrum Potsdam,
Telegrafenberg, 14473 Potsdam, Germany
E-mail: romer@gfz-potsdam.de

Editorial responsibility: J. Hoefs

Description of the problem

The decay of ^{238}U and ^{235}U to ^{206}Pb and ^{207}Pb, respectively, involves a series of α decays. The preservation of

impulse requires that radioactive decay resulting in the emission of particles induces a recoil on the nucleus. The recoil distance depends on the mass and the energy of the emitted particle (e.g., Ziegler et al. 1985). Alpha-decays in the ^{238}U and ^{235}U decay series yield recoil distances in zircon ranging from 208 to 329 Å (e.g., compilation in Nasdala et al. 2001). These distances are several times larger than the distance to the nearest neighbors and corresponds for zircon in a displacement of about 30–50 unit cells. Thus, the daughter nucleus formed by α-decay will be at a different location than the one originally occupied by the parent nucleus. For the ^{238}U and ^{235}U decay series, α-recoil can amount to a maximum displacement of 2,040 and 1,900 Å (i.e., each incremental displacement is aligned) for ^{238}U (eight α-decays) and ^{235}U (seven α-decays), respectively. Because of the random nature of the direction of recoil, most ^{206}Pb and ^{207}Pb daughter nuclei, however, will be displaced a much smaller effective distance from the site of their U-parents.

To understand how α-recoil affects the parent-to-daughter system (P/D) of a mineral, consider the following two schematic scenarios: A mineral has a homogeneous P distribution and another mineral has a highly heterogeneous P distribution (Fig. 1). D is displaced by α-recoil by a distance much smaller than the diameter of the mineral sample and is not redistributed by secondary processes (cf. also ''internal reverse discordance'' vs. ''external reverse discordance'' in Mattinson et al. 1996). Thus, in a homogeneous sample (i.e., identical P contents in each subvolume) the amount of D lost from a subvolume is identical to the amount of D gained. Despite the displacement of D and the obvious open-system character of the example, the P/D system displays perfect closed-system behavior on the scale of the selected subvolume. There is no excess or deficit of D, but for the crystal margins where loss to or gain from the surrounding may have occurred. For a heterogeneous volume, such as a crystal with oscillatory zoning or with inclusions, the contacts between the two chemically different materials may be characterized by a deficit or excess of D in a zone approximately as wide as the recoil displacement. Those segments with higher contents of P eventually lose more D than they receive from adjacent volumes, whereas the adjacent areas of low P contents develop a D excess. The magnitude of the developing deficit and excess in D depends on the contrast in P content between the two segments. The larger the contrast, the larger is the anomaly. This relation is shown schematically in Fig. 1.

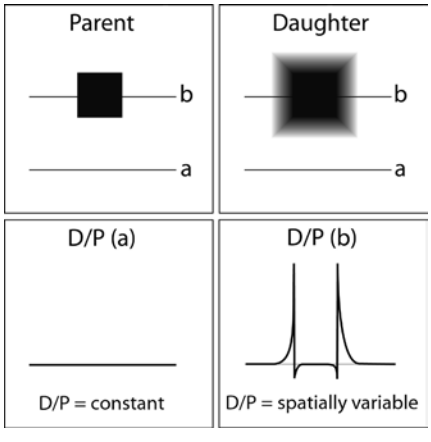

Fig. 1 Parent (*P*) and daughter (*D*) isotope distribution in a heterogeneous mineral. *a* and *b* represent two hypothetical profile lines along which the *D*/*P* ratio is determined. For a profile across an area with homogeneous parent distribution (*a*), D/P is constant despite the random redistribution of the daughter. In the border zone between two areas of contrasting P content (*b*), variations occur in D/P. There is a deficit of D in the area of high P and there is an excess of D in the area of low P. Note that the excess of D may represent a much larger portion of a subsample than the D deficit

In systems used for geochronology, variations in D/P (Fig. 1) correspond to variations in age (for $D_0 = 0$). For large sampling volumes that encompass the entire inclusion and its halo of α-recoil induced redistribution of D, the observed D/P is identical to the one of the homogeneous host-crystal of identical age, as long as the inclusion and host are coeval. Reducing the sample volume may result in situations where only the homogenous crystal or the inclusion is sampled. As long as the sampled volume is far from the interface between host and inclusion, D/P is identical for all subvolumes. Near the interface, however, samples from the P-rich inclusion yield slightly too low D/P, whereas samples from the P-poor host yield distinctly too high D/P (Fig. 1).

Recoil and the requirement of a closed system at a first look seem mutually incompatible as recoil of the daughter nucleus by definition implies an open system on the nanoscale. On a larger scale, however, α-recoil results in a redistribution of daughter isotopes within the sampled volume. The U–Pb systematics represent a closed system as long as the sampled volume is large in comparison to the displacement by recoil and did not experience a loss or gain of mobilized daughter isotopes through secondary processes. The questions addressed in this paper are (1) whether there are analytical approaches that probe volumes sufficiently small to be affected by recoil-induced isotopic and concentration effects and (2) how such effects may appear and eventually be recognized.

Recoil distance versus sample size: a comparison of scale

Displacement of D by α-recoil is in the range of a few hundred Ångström and does not reach beyond 0.2 μm even for the most unlikely geometric combinations of recoils in the decay series of ^{238}U, ^{235}U, and ^{232}Th. This is much smaller than the size of typically dated crystals. Air-abrasion (Krogh 1982b) removes the outermost parts of zircon that may have experienced Pb-loss to the surrounding of the crystal and may also remove mechanically less resistant, metamict domains. Thus, as long as loss of the daughter isotope through the crystal surface can be eliminated, α-recoil has little or no effect

on the U–Pb systematics of bulk samples of single crystals or population of crystals. The use of an ion-microprobe (SHRIMP, Cameca) or laser-ablation (LA-MC-ICP-MS) to introduce material into the mass spectrometer typically samples spots of 25–35 μm in diameter and pits of 50×50 μm, respectively. Sputtered and ablated areas typically are 5–10 μm deep. These sample volumes are large in comparison to the displacement of the daughter isotopes by α-recoil. Therefore, anomalous features (e.g., reverse discordance) can hardly be attributed to the spatial separation of parent and daughter isotopes in sample with a highly heterogeneous distribution of the parent. The only analytical approach that has a spatial resolution approaching the dimension of the displacement by α-recoil is leaching and step-wise selective dissolution (cf. Mattinson 1994; Mattinson et al. 1996). The preferential dissolution of inclusions and chemically contrasting parts of a crystal may result in subsamples that have similar effective dimensions as the displacement by α-recoil. Furthermore, the carving of non-annealed fission tracks may create a spongy, highly porous residual crystal that allows the fractionation of P and D from a much larger volume than prescribed by the scale of the chemical heterogeneities. The P/D system of such chemically and structurally heterogeneous systems may become disturbed by step-wise dissolution in a systematic and predictable, yet difficult to quantify manner.

Effect of α-recoil on samples with heterogeneous U and Th distribution analyzed by stepwise dissolution

Leaching or stepwise dissolution can reduce the discordance of a sample by preferentially dissolving metamict sections and inclusions (e.g., Mattinson 1994; McClelland and Mattinson 1996; Romer and Wright 1992; Romer et al. 1996) or increase the range of Pb isotopic variability to better define Pb–Pb lines using a set of subsequent leaching steps (e.g., Frei et al. 1995, 1997). These procedures are highly successful in some cases (e.g., Mattinson 1994; McClelland and Mattinson 1996; Frei et al. 1995, 1997; Romer and Smeds 1996) and yield anomalous data pattern in other cases (e.g., Romer et al. 1996; Corfu 2000; Davis and Krogh 2000). In the following, the examples of (1) oscillatory, chemically zoned zircon, (2) uraninite inclusions in columbite-tantalite, and (3) micro-inclusions of zircon and monazite in, e.g., staurolite, kyanite, and garnet are used to argue that anomalous data patterns originating from leaching are essentially confined to samples with highly heterogeneous U and Th distribution.

Zircon

Sample treatment with dilute or concentrated acids can result in the selective dissolution of metamict or chemically distinct sections of a mineral. Common to most leaching procedures is the fact that late leaching steps produce data that are slightly discordant or even concordant, whereas early leaching steps show pronounced disturbance and anomalous isotope signatures—first described for zircon mostly by Mattinson (1997) and later confirmed by other groups—including (1) reverse discordance (e.g., Todt and Büsch 1981; Davis and Krogh 2000; Chen et al. 2002), (2) lower $^{207}Pb_{rad}/^{206}Pb_{rad}$ in early leachates than for the concordant residues (e.g., Corfu 2000; Chen et al. 2002); (3) higher $^{207}Pb_{rad}/^{206}Pb_{rad}$ in intermediate leachates than for the concordant residues (e.g., Corfu 2000); (4) negative lower discordia-intercept ages (e.g., Davis and Krogh 2000), and (5) preferential mobilization of ^{234}U over ^{238}U (Davis and Krogh 2000). Some of these anomalous effects have been discussed in terms of analytical artifacts, some as effects of processes on the nanoscale, and others as results of the thermal history of the dated rocks (e.g., Todt and Büsch 1981; Mattinson 1994; Corfu 2000; Davis and Krogh 2000). For instance, reverse discordance may reflect Pb-U fractionation through the precipitation of fluorides (e.g., Mattinson 1994). Mattinson at al. (1996) suggested that reverse discordance also may be induced by α-recoil resulting in Pb loss from U-rich zones, eventually giving rise to Pb excess in U-poor zones, which are more resistant to leaching. Alpha-recoil has been also invoked as cause for preferential mobilization of ^{234}U over ^{238}U (Mattinson 1997; Davis and Krogh 2000) and the fractionation of $^{206}Pb_{rad}$ and $^{207}Pb_{rad}$ (Mattinson 1997) during leaching. Effects originating from recoil processes may be superimposed by Pb segregation in zircon subdomains during thermal annealing episodes early after zircon crystallization (Corfu 2000; Davis and Krogh 2000). This concept of early thermal annealing of damages induced by α-recoil in combination with anomalous $^{207}Pb_{rad}/^{206}Pb_{rad}$ signatures was even used to estimate an annealing temperature of 200–300 °C and to constrain the exhumation and cooling history of rocks (Davis and Krogh 2000).

The above anomalous features of the U–Pb systematics revealed by leaching have been described for zircon samples with heterogeneous U–Th distribution, chemical zoning, and inclusions (e.g., Todt and Büsch 1981; Mattinson 1994; Mattinson et al. 1996; Corfu 2000; Davis and Krogh 2000), which allow a separation of the ultimate daughter isotopes (Pb) from their parents (U, Th) into a chemically different environment. The effect of the spatial separation of parent and daughter isotopes on the geochronological system of the dated material may become analytically resolvable if there are pronounced U and Th concentration differences between adjacent, chemically contrasting zones, as well as inclusion and host, and if heterogeneities occur on a similar scale as the recoil distance. The finer the chemical zonation and the smaller the inclusions, the larger the likelihood that recoiled daughter isotopes are ejected from a zone or inclusion into a zone of contrasting composition and leaching behavior. Backscattered electron images and cathodoluminescence studies (e.g.,

Hanchar and Miller 1993; Vavra et al. 1996, 1999; Goetze et al. 1999) showed that the width of chemically contrasting oscillatory bands may be in the micron to sub-micron range. Similarly, raster electron-microscope images of leached and partially dissolved zircon (Fig. 2) reveal that selective dissolution may sculpture crystals into highly porous material at the micron to submicron scale (e.g., Claesson and Williams 1987; Mattinson 1994; Mattinson et al. 1996). Thus, chemical heterogeneities within individual zircon crystals and their selective dissolution may have similar dimensions as the recoil-distance of U-daughter isotopes in zircon (cf. compilation in Nasdala et al. 2001).

Sequential dissolution preferentially removes U-rich bands that are characterized by a recoil-induced deficit in radiogenic Pb. The U–Pb systems of the solutions are discordant, show a too-young apparent $^{207}Pb/^{206}Pb$ age in comparison with the concordant sample, and are possibly best described by a continuous Pb-loss model comparable to the ones of Tilton (1960) and Wasserburg (1963). The residue of this first dissolution-step commonly is reversely discordant. Subsequent leaching steps preferentially dissolve zircon bordering the U-rich zones. These zones show a recoil-induced Pb-excess, which, in combination with a higher extent of recovery of old recoil damages, results in too-old apparent $^{207}Pb/^{206}Pb$ ages relative to the concordant sample. Only the most severely leached residues that are devoid of U-rich zones and their adjacent veneers of Pb excess may yield concordant data (cf. Mattinson 1994; McClelland and Mattinson 1996; Corfu 2000), provided they have a rather homogeneous content of U and they are not smaller than several microns.

Stepwise leaching reveals the superimposed effects from two different processes, recoil implantation and preferential mobilization from structurally damaged domains. Step-wise leaching may reveal in individual leachate or residual factions reverse discordance and Pb-isotope fractionation. The relative portion of contributions from recoil implantation and preferential mobilization from structurally damaged regions may vary during the leaching procedure and depend also on the accumulated radiation damage, which depends on age and U,Th content of the sample, as well as on its thermal history.

Reverse discordance. Atomistic modeling of α-recoil suggests that the most intense structural damage caused by collision cascades occurs in an elongated volume near the original location of the parent isotope, whereas the daughter isotope may reside in a structurally less disturbed volume (Trachenko et al. 2001). Each of these collision cascades represents a small metamict volume that is shielded from interaction with the surrounding by structurally intact zircon. The superposition of collision cascades through subsequent recoils eventually may yield connected areas that may interact with the surrounding of the crystal. Such interaction may be additionally aided by α-tracks and especially fission-tracks. Step-wise dissolution may cause reverse discordance of the residue through (1) preferential dissolution of the structurally most damaged areas and (2) recoil-implantation of the daughter isotope into an environment of

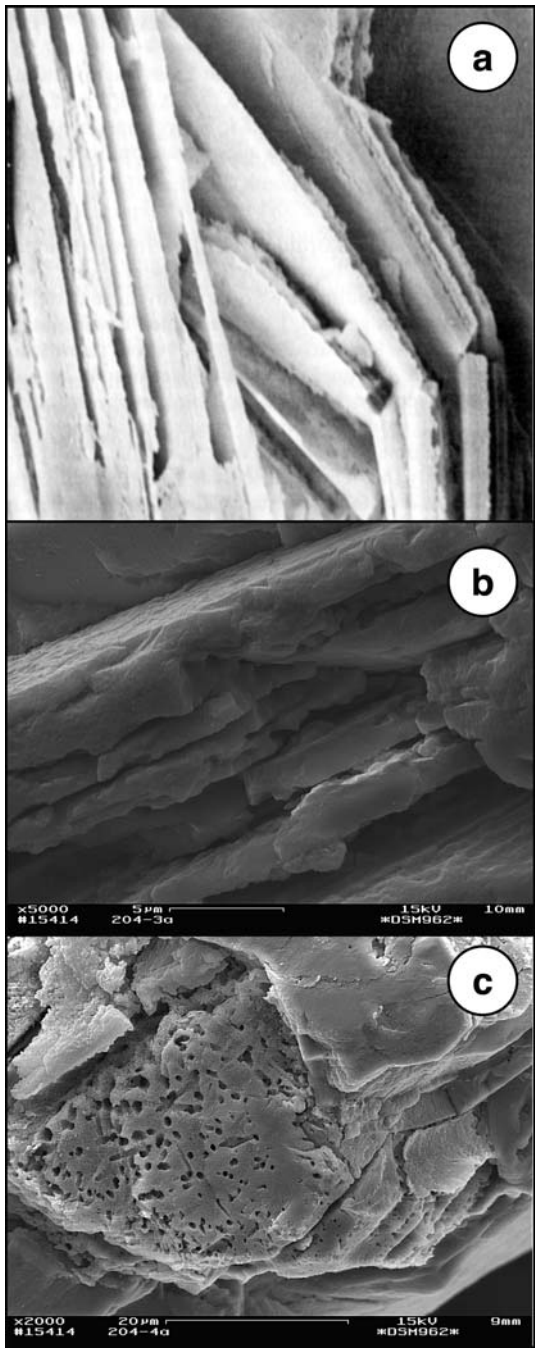

Fig. 2 REM images of leached zircon to illustrate the fine scale of features sculptured by selective leaching. **a** Leached zircon. Width of field of view: ca. 8 µm (from Mattinson 1994). **b** Leached zircon showing irregular excavation of U-rich layers. Note that U-poor shells, fractured through expansion of underlying metamict material, break off at the contact to U-rich zones. Width of field of view: ca. 25 µm [from Littmann (Potsdam), unpublished]. **c** Leached zircon. View on a U-poor layer. The overlying U-rich layer has been dissolved. Holes in the U-poor layer represent fission tracks emanating from the U-rich layer. Width of field of view: ca. 60 µm [from Littmann (Potsdam), unpublished]

chemical contrasting behavior. Areas with the highest contents of U are those that acquired most structural damage and, thus, are among the volumes dissolved during early dissolution steps. Reverse discordance in the residue implies that there is a preferential loss of U over Pb_{rad}, i.e., that recoiled Pb is less mobilized than U in the metamict areas damaged by recoil cascades. Excess originating from recoil-implantation may be found in residues of late-dissolution steps, i.e., low Th,U domains (Mattinson et al. 1996).

Pb-isotopic fractionation. Anomalous apparent $^{207}Pb/^{206}Pb$ ages for the first dissolution steps have been described in numerous studies (e.g., Mattinson 1994; Mattinson et al. 1996; Corfu 2000). Whereas too-old apparent $^{207}Pb/^{206}Pb$ ages may be explained by the preferred dissolution of old cores (e.g., Mattinson 1994; Mattinson et al. 1996), too-young apparent $^{207}Pb/^{206}Pb$ ages in leachates from core-free zircon samples have been explained by (i) contrasting levels of annealing of old and young recoil tracks (e.g., Davis and Krogh 2000; Corfu 2000), (ii) higher sampling efficiency from zones of higher structural damage causing a preferential sampling of young $^{206}Pb_{rad}$ and $^{207}Pb_{rad}$, eventually resulting in discordia systems with negative lower intercepts (Mattinson 1997), and (iii) the spatial separation of $^{206}Pb_{rad}$ and $^{207}Pb_{rad}$ due to the variation in recoil distance for each kind of α-decay and the different number of α-decays in the two decay series (eight α-decays for ^{238}U and seven α-decays for ^{235}U). These three possible explanations are based on the same process, i.e., the displacement and structural damage through α-recoil, but focus on contrasting aspects. Explanation (1) was suggested for old zircon samples, where the "instantaneous" $^{207}Pb_{rad}/^{206}Pb_{rad}$ had been lowered significantly with increasing time. This explanation suggests that thermal annealing of structural damages may have progressed further for old damages than for younger ones (Davis and Krogh 2000), which implicitly requires that there was a later reheating event or the rocks remained buried for a prolonged time. Such an explanation, however, may not be able to explain the variation in $^{207}Pb_{rad}/^{206}Pb_{rad}$ in young zircon samples. Explanation (2) focuses on the role of contrasting levels of structural damage for the mobilization of $^{207}Pb_{rad}$ and $^{206}Pb_{rad}$. By indirectly linking the age of a sample with its U content, emphasis is put on the spatial distribution of U and the possibility that the increasing extent of structural damage may reduce the ability to anneal (cf. Geisler et al. 2001; Geisler 2002). Explanation (3) focuses on the spatial separation of $^{207}Pb_{rad}$ and $^{206}Pb_{rad}$ and the larger total displacement and energy released for $^{206}Pb_{rad}$ than for $^{207}Pb_{rad}$, which translates into a higher probability for recoil-damages associated with $^{206}Pb_{rad}$ to intersect with long-range damages, such as α-tracks and fission-tracks, than for those related with $^{207}Pb_{rad}$. This renders $^{206}Pb_{rad}$ more leachable and eventually results in too low $^{207}Pb_{rad}/^{206}Pb_{rad}$ in the leachate.

Cumulative radiation damage. Depending on age, Th,U content, and thermal history, zircon may have acquired a wide range of cumulative radiation damage. The increasing cumulative damage correlates with changes in interconnection and superposition of radiation damages. At low cumulative radiation damage, the various domains of recoil-induced metamictization occur isolated in crystalline material. The dissolution and leaching behavior is largely dominated by the properties of the structurally intact zircon. At higher radiation damage, the various metamict domains interconnect to a network, possibly enhanced by the distribution by the much rarer, yet considerably longer fission-tracks. The dissolution and leaching behavior of zircon is controlled by transport properties along the structurally damaged zones (cf. also Petit et al. 1989; Geisler et al. 2001). Eventually, cumulative radiation damage reaches a stage of large interconnected metamict domains with isolated rafts of lesser damage. The dissolution and leaching behavior of this zircon is dominated by the metamict material. Therefore, cumulative radiation damage eventually influences properties of the crystal in annealing and leaching experiments (e.g., Murakami et al 1991; Weber 1994; Geisler et al. 2001; Nasdala et al. 2001; Geisler 2002). Above explanations for reverse discordance and the fractionation of $^{207}Pb_{rad}/^{206}Pb_{rad}$ through sequential leaching experiments all may apply to individual samples, although depending on cumulative radiation damage, as well as the temporal variation of accumulation (which reflects the thermal history of the sample), different processes may predominate for a young or old zircon, for U-rich or U-poor zircon.

Columbite–tantalite–tapiolite

The U–Pb systems of columbite–tantalite–(tapiolite) in many samples are a combination of the U–Pb systems of the pure columbite–tantalite host and those of its inclusions. Abundant inclusions of bismuthite, uraninite, rutile, cassiterite, but also of quartz and feldspar, as well as alterations to, and intergrowth with, ixiolite, fersmite, microlite, betafite, and pyrochlore-group minerals have been demonstrated from many columbite-tantalite occurrences (e.g., Cerny et al. 1989; Romer et al. 1996; Uher et al 1998; Tindle and Breaks 1998; Tindle et al. 1998). Leaching of columbite-tantalite in dilute HF results in the dissolution of uraninite, sulfide, and silicate inclusions, as well as the partial dissolution of their host. The HF-leaching generally increases $^{206}Pb/^{204}Pb$, through preferential removal of common Pb bound in sulfides and feldspar inclusions, and decreases the discordance of the U–Pb systems (samples washed in 7 N HNO_3 and 6 N HCl are commonly reversely discordant). Leaching with more concentrated acids yields less discordant and eventually concordant data (e.g., Romer and Wright 1992; Romer and Smeds 1994, 1996, 1997). In many cases, the most severely leached samples (and now highly porous crystals, Fig. 3; Romer and Smeds 1996) yield concordant data, whereas non-leached samples yield strongly reverse discordant data (e.g., Aldrich

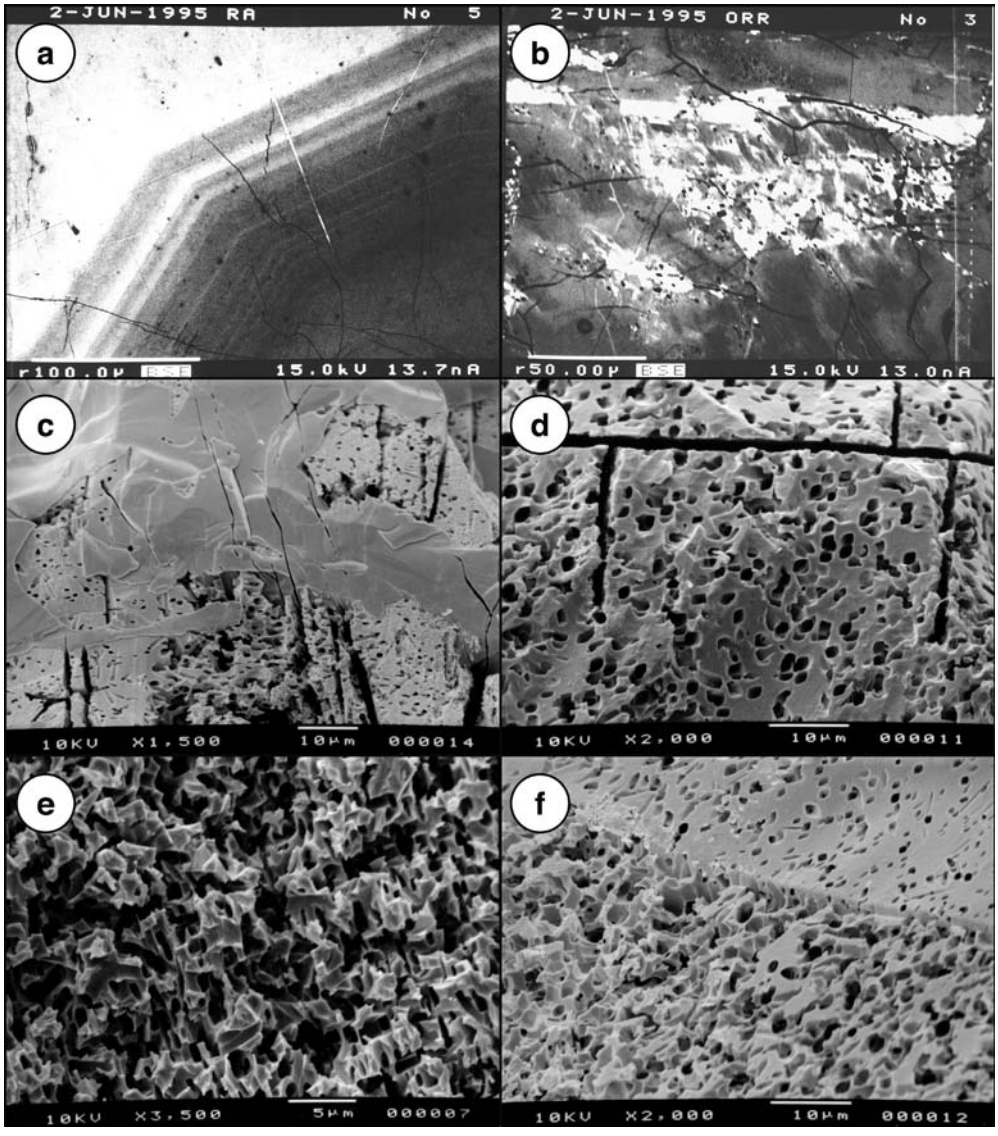

Fig. 3 BSE (**a**–**b**) and REM (**c**–**f**) images of columbite-tantalite to illustrate the fine scale of primary magmatic heterogeneities and the highly selective behavior during HF-leaching. **a** Oscillatory growth zonation reflected in contrasting Ta (*bright*) and Nb (*dark*) contents (Rånö location; Romer et al. 1996). **b** Secondary Ta-rich Nb,Ta-oxides along fractures (*white lines*) and as replacements (*white irregular patches*). If such phases formed in the late-magmatic stage of pegmatite crystallization, they would have had little or no effect on the U–Pb systematics. If the replacement is related to a much later event, it may result in a fractionation of U and Pb and make reverse discordance permanent (Orrvik location; cf. Romer and Smeds 1994). **c**–**f** HF-leached Sveconorwegian columbite–tantalite samples that yield concordant U–Pb data (Romer and Smeds 1996). Fractures originally filled with quartz or feldspar have been mined-out during HF-leaching. *Small dots* and *grooves* are fission-tracks and directly reflect the distribution of U between Nb-rich (few tracks) and Ta-rich (numerous tracks) columbite-tantalite. For an age of 1 Ga and 200 ppm U, there may be as many as 140 fission tracks in a volume of 5 µm by 10 µm by 10 µm. The number of tracks may be reduced through thermal annealing. **c** Timmerhult location: 140–225 ppm U in HF-leached fractions (**d**) Skantorp location: 162–186 ppm U in HF-leached fractions (**e**) Riddaho location: 790–1,270 ppm U in HF-leached fractions (**f**) Skantorp location: 162–186 ppm U in HF-leached fractions

et al. 1956; Romer and Smeds 1994, 1996). A suite of variably HF-leached samples commonly defines a discordia intersecting the concordia at the age of columbite–tantalite formation and the origin of the concordia diagram with little excess scatter about the discordia. There are, however, also columbite–tantalite samples that yield excess scatter about the discordia or along a short segment of the concordia (Fig. 4) or that define a discordia with a negative lower intercept (e.g., Romer and Smeds 1997). These samples generally are characterized by the occurrence of uraninite inclusions (Romer et al. 1996).

The excess scatter selectively associated with samples that have uraninite inclusions suggests that the inclusions play an important role in establishing the scatter. Since the inclusions are removed during leaching, the persistence of anomalous $^{207}Pb_{rad}/^{206}Pb_{rad}$ is not restricted to the uraninite inclusion itself, but to its nearest environment in columbite that is not necessarily removed during leaching. Columbite-tantalite

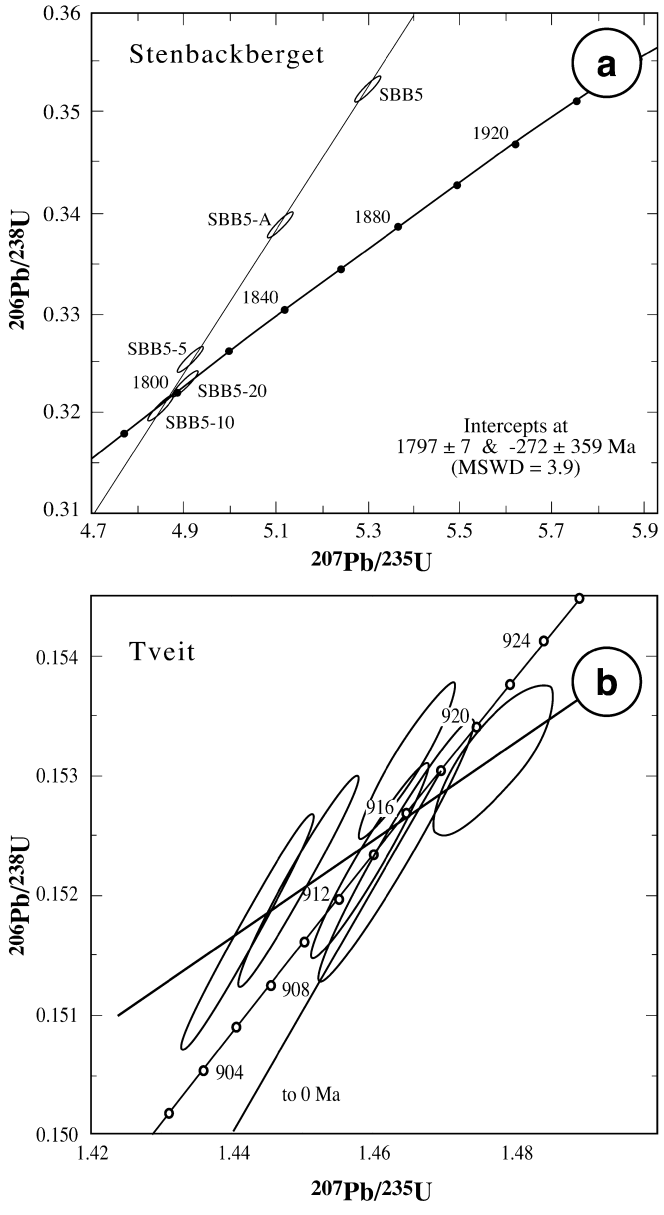

Fig. 4 U–Pb columbite data illustrating heterogeneities originating from uraninite inclusions. **a** Strong reverse discordance that is reduced through leaching. SBB5 and SBB5-A: acid wash with 7 N HNO_3 and 6 N HCl; SBB5-5: acid leach with 5% HF; SBB5-10: acid leach with 10% HF; SBB5-20: acid leach with 20% HF. Excess scatter and negative lower intercept are defined by the least leached or not leached samples (Data source: Romer and Smeds 1994). **b** Concordant to subconcordant U–Pb data from repeatedly leached columbite samples. All leaches with 20% HF (Data source: Romer, Pedersen, and Raade: unpublished data)

in direct contact with the uraninite inclusion received important amounts of $^{207}Pb_{rad}$ and $^{206}Pb_{rad}$ implanted through α-recoil. This recoil-implantation produces a small damage cluster by collision cascades of displaced atoms, (e.g., Weber et al. 1994) that may start to anneal already at low temperatures (e.g., Murakami et al. 1991; Meldrum et al. 1998; Nasdala et al. 2001). Thus, later acid treatment may leach implanted daughter isotopes of the Th–U decay chains only if they occur on the crystal surface or the recoil path has not annealed yet. This could eventually result in the preferential removal of late-generated radiogenic Pb (see also Davis and Krogh 2000). Implanted Pb with annealed recoil-tracks may remain in the columbite host. Due to the large contrast in U content in columbite and uraninite, there is considerably higher Pb-implantation into columbite than Pb-loss from columbite. Reverse discordance during early leaching stages is related to recoil-implantation and is enhanced through the preferential dissolution of the structurally most damaged domains, i.e., the domains turned metamict by recoil cascades (e.g., Weber et al. 1994; Meldrum et al. 1998). Since the volumes with most recoil cascades also are those with the highest U content, acid washing and early leaching steps may remove those sections and, thereby, enhance the reverse discordance. The excess scatter originates possibly from (1) polystage evolution of uraninite, (2) the preferential annealing of old tracks, and (3) the uncoupling of $^{207}Pb_{rad}$ from $^{206}Pb_{rad}$ during recoil processes. The $^{207}Pb_{rad}/^{206}Pb_{rad}$ values of leached residues may differ significantly from the $^{207}Pb_{rad}/^{206}Pb_{rad}$ value of the concordant sample (Fig. 4) and if used to constrain the discordia may result in too-young (even negative) lower intercepts with the concordia (Fig. 4).

Rock-forming silicates

Stepwise leaching of, e.g., staurolite, garnet, and kyanite is thought to dissolve sequentially crystal domains of different crystallinity and chemical signature (e.g., Frei et al. 1995, 1997) or to remove inclusions selectively by dissolving them or by enriching them in the residue (e.g., Frei et al. 1997; Dahl and Frei 1998). For most silicate phases, the effect of daughter-isotope redistribution by α-recoil may be subordinate as long as the leached mineral is a U-poor phase that does not show orders of magnitude variations in U content. For such minerals, Pb loss and Pb gain are comparable and should not affect the geochronological system to the extent of analytical resolvability. Micro-inclusions of U-rich and Th-rich phases, such as monazite, xenotime, and zircon, however, may represent micro-environments where the Pb loss through α-recoil from the inclusion far exceeds the Pb gain from the host. The preferential dissolution of monazite or xenotime eventually leaves behind an excess of radiogenic Pb in the silicate residue. To which extent the fractionation of U and Pb during this leaching step also results in contrasting $^{207}Pb_{rad}/^{206}Pb_{rad}$ between dissolved monazite and silicate residue depends on the magnitude of contrasting implantation of $^{207}Pb_{rad}$ and $^{206}Pb_{rad}$, the size of the inclusion in comparison to the average recoil distance, and furthermore on the healing behavior of the damage along the recoil path and in the near-environment of the recoiled nucleus. If old damage is recrystallized to a higher extent than young damage, for instance due to prolonged residence in the middle or

lower crust or reheating during a second event, early formed nuclei are more likely to have been incorporated in the crystal structure of the host minerals than recently recoiled nuclei. For such samples, there may be a fractionation between $^{207}Pb_{rad}$ and $^{206}Pb_{rad}$ (cf. also Davis and Krogh 2000) that is due to the changing production rate of $^{207}Pb_{rad}$ and $^{206}Pb_{rad}$ through time. Thus, if early recoiled Pb is retained in the silicate residue to a higher extent than later recoiled Pb, the silicate residue has an excess of ^{207}Pb and the solution has a slight deficit in ^{207}Pb. During later dissolution steps, a similar Pb-deficit may be found in residual zircon, whereas the leach solution has a Pb excess. Due to the highly correlated nature of $^{207}Pb/^{204}Pb$ and $^{206}Pb/^{204}Pb$, such recoil effects do not necessarily result in excess scatter among subsequent leach steps in the $^{206}Pb/^{204}Pb$–$^{207}Pb/^{204}Pb$ diagram. They may, however, become apparent in a variation in $^{206}Pb/^{238}U$ ages of subsequent dissolution steps that all scatter within a range of a few percent about the correct age (e.g., Frei et al. 1997), which could reflect either fractionation of U and Pb during leaching (i.e., an artifact from sample treatment) or recoil-induced U and Pb fractionation.

Radiation damage and element mobilization: structural and energetic controls

Visualization of α-tracks and fission-tracks (Fig. 3c–f) through preferential dissolution of material affected by radiation damages illustrates: (1) structurally damaged domains are sources (or sinks) of material. They represent volumes of higher reactivity and higher ion-exchange potential than structurally intact volumes; (2) the dissolution behavior is controlled by mineral chemistry and damage density; (3) tracks represent pathways for fast transport of material from the interior of the crystal to the surface. These qualitative and intuitive relations have been characterized and quantified in numerous infiltration, reaction, and structural-recovery experiments. For instance, leaching experiments on old zircon samples demonstrate a systematic relationship between reaction-rim thickness and cumulated α-dosage (e.g., Geisler et al. 2001), reflecting the higher potential for chemical exchange in metamict than in crystalline material. Similarly, infiltration rates have been shown to be higher for damaged silicate structures than for undamaged ones (e.g., Petit et al. 1989).

The densities of α-damages and fission-tracks due to the decay of U are highly correlated through the decay constants. They depend on the U content and the age of the samples. Volumes of high density of α-damage, i.e., enhanced reactivity and facilitated element mobilization, also are volumes of high track density, i.e., large-scale crystal defects that allow for fast transport. The control of damage distribution on material properties, such as elemental mobilization and long-range transport through crystalline matter, implies that both the age of a sample and its enhanced contents of U and Th affect the values of these material properties. Consequently, old crystalline material should have higher diffusivities and leachability than young or synthetic material of identical chemical composition. This damage-related variation of mineral properties is not restricted to elements pertinent for dating, but applies to all elements.

Accumulated structural damage also may reduce the activation energy required to sputter or ablate material from zircon or columbite and may, thereby, give rise to a non-stoichiometric mobilization of U and Pb different from the one obtained on external standard material. For instance, Black et al. (1991) and Wiedenbeck (1995) demonstrated excess of radiogenic Pb in SHRIMP spot-analyses of U-rich zircon even though the conventional bulk analysis of the same material gave normally discordant or concordant U-Pb data. The fact that SHRIMP data align along a chord through the origin of the diagram was interpreted to reflect an analytical aberration reflecting different sputtering efficiencies of Pb and U in the zircon standard and the analyzed U-rich zircon sample (Black et al. 1991) or the sampling of labile Pb from strongly damaged zircon (Wiedenbeck 1995). Smith (2001) presented LA-MC-ICP-MS U–Pb data from columbite-tantalite that align along chords generally passing through the origin of the concordia diagram. The data plots are reversely discordant, except for spots from one sample. There is an overall negative correlation between U content and excess age. The preferential mobilization of Pb implanted from U-rich zones into U-poor zones may explain both reverse discordance and the higher age excess in spots with lower U content.

This anomalous behavior of some zircon and columbite-tantalite samples subjected to analysis by ion-probe or laser-ablation may be controlled by the distribution of fission-tracks and α-tracks rather than the distribution of damage accomplished by α-recoil collision cascades. Although all three kinds of damage are related to U, the distribution of fission and α tracks differs slightly from that of α-recoil damage due to the contrasting range of the various damages. In zircon, fission tracks are typically 10–11 μm long (Tagami et al. 1996), α-tracks range from 10–25 μm depending on the energy of the α-particle (Nasdala et al. 2001), whereas α-recoiled nuclei travel only some 200–330 Å (cf. Nasdala et al. 2001). Deep-reaching tracks represent pathways that make recoiled Pb accessible for leaching or thermally-activated migration from a much larger volume than the zone bordering the U-rich segment that is affected by heavy α-recoil. The extent to which recoiled Pb from U-poor zones is mobilized depends on the overall distribution of long tracks, i.e., on the distribution of U, the annealing behavior of tracks, and the thermal history of the sample. Leached, sputtered, or ablated samples that show a high density of fission and α tracks may show a higher excess of radiogenic Pb than samples with a low density of damages.

Influence of annealing and recrystallization on the U–Th–Pb systematics of heterogeneous samples

Annealing of defects, the formation of secondary phases (e.g., Fig. 3b) of similar leaching behavior as the primary mineral, or open system behavior due to weathering and hydrothermal leaching make the spatial separation of daughter and parent isotopes permanent. Mattinson (2000) demonstrated for single-stage U–Pb systems of zircon that most of the Th–U–Pb fractionation and preferential mobilization of Pb with too-old or too-young apparent $^{207}Pb/^{206}Pb$ ages can be avoided by annealing the α-recoil damage and fission tracks in the laboratory before step-wise dissolution. High-temperature annealing in the laboratory may also remove possible effects of cumulative radiation damage on the non-stoichiometric sputtering and ablation behavior during SHRIMP and LA-MC-ICP-MS spot analysis, respectively.

Mattinson (2000, 2001) notes that problems associated with annealing in the laboratory may include redistribution of Pb by diffusion and Pb loss by volatilization during high-temperature annealing. Pb mobilization before or in conjunction with annealing and recrystallization—if related to a distinct thermal event, weathering, or exposure to a Ca-rich thermal fluid (e.g., Kurz 2000; Geisler et al. 2001) in the past—may significantly affect the potential to extract an age from a data set. Renewed accumulation of radiation damage makes ions, which were immobilized by annealing or the formation of secondary phases, again available for redistribution. By such a mechanism, an anomalous discordia could be arbitrarily transposed to higher $^{206}Pb_{rad}/^{238}U$, eventually resulting in an upper intercept age that is too-young by some Ma and a lower intercept age that is without geological significance (Fig. 5).

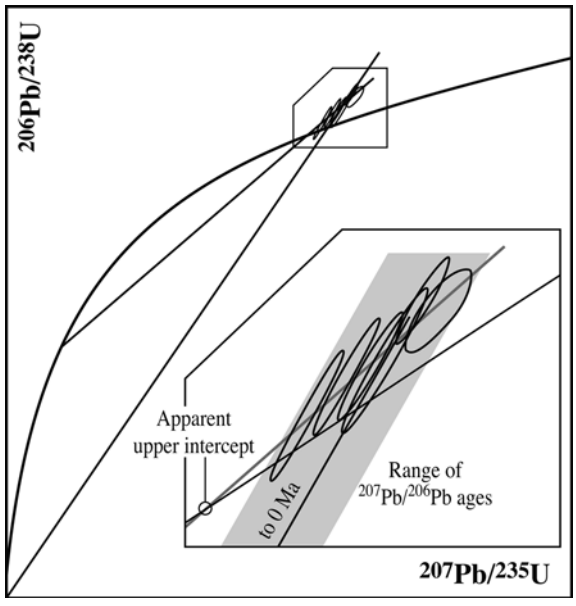

Fig. 5 Schematic concordia diagram showing a sample set that became reversely discordant, annealed at some time, and acquired additional reverse discordance. Stepwise dissolution removes only part of the reverse discordance. The discordia may be displaced to high $^{206}Pb_{rad}/^{238}U$ values and therefore intercept the concordia at a too young upper intercept and an arbitrary (possibly too old) lower intercept

Summary and conclusions

Alpha-decay results in the displacement of the daughter nucleus by some 200–330 Å and the cumulation of structural damages that are associated with collision cascades caused by the recoiled nucleus and to a lesser extent with the α-track. The decay series starting from ^{238}U, ^{235}U, and ^{232}Th result in Brownian-type displacement of a series of recoiled daughter nuclei reaching a total displacement of 0.1–0.2 μm. Recoil results in a contrasting spatial distribution of parent and daughter and contrasting level of structural damage that may result in contrasting mobilization of U and Pb from zones of high and low recoil damage. This can cause anomalous data patterns in analytical schemes with high spatial resolution or with extraction volumes sensitively controlled by activation energies, such as for leaching, SHRIMP, or LA-MC-ICP-MS analysis.

Geometric effects may be revealed by leaching and step-wise dissolution that can reach narrow zones. Selective chemical extraction generally starts with the preferential removal of U and radiogenic Pb from parts of the mineral strongly damaged by α-recoil collision cascades, α-tracks, and fission tracks. Later dissolution steps may yield increasingly more concordant data. Implantation of Pb into an environment of contrasting leaching behavior and preferential annealing of old damage during the thermal history of the rock may give rise to anomalous $^{207}Pb_{rad}/^{206}Pb_{rad}$. The magnitude of anomalous behavior during step-wise dissolution depends on the magnitude of chemical heterogeneity in terms of scale and range of contents. Small-scale open-system behavior due to α-recoil has no effect on bulk analyses as long as there had been no selective attack of chemically different domains of a mineral, which could have caused U-Pb fractionation, through weathering, recrystallization, or medium-to-high temperature metamorphic fluids.

In SHRIMP and LA-MC-ICP-MS analysis, the anomalous behavior of the U-Pb system originates from contrasting activation energies of (1) structurally bound (annealed) and labile Pb (recoiled Pb) and (2) of U and Pb from structurally intact or heavily damaged segments of the mineral, which eventually provides for excess by activating a larger volume for Pb than for U. Additional isotopic fractionation between $^{207}Pb_{rad}$ and $^{206}Pb_{rad}$ originating from the annealing history of a sample might be present, but is commonly far beyond analytical resolution. For single-stage geologic histories, this effect may be reduced or removed by annealing the samples before analysis.

Acknowledgements I thank Sten Littmann (GFZ Potsdam) for Fig. 2b, c. The SEM images of leached columbite-tantalite crystals were made by Ulf Sturesson (Uppsala) in the course of an earlier project (with Sten-Anders Smeds, Uppsala). I am grateful to James M Mattinson (Santa Barbara) and Fernando Corfu (Oslo) for detailed and constructive reviews.

References

Aldrich LT, Davis GL, Tilton GR, Wetherill GW (1956) Radioactive ages of minerals from the Brown Derby Mine and the Quartz Creek Granite near Gunnison, Colorado. J Geophys Res 61:215–232

Black LP, Kinny PD, Sheraton JW (1991) The difficulties of dating mafic dykes: an Antarctic example. Contrib Mineral Petrol 109:183–194

Chen F, Siebel W, Satir M (2002) Zircon U-Pb and Pb isotope fractionation during stepwise HF acid leaching and geochronological implications. Chem Geol 191:155–164

Cerny P, Chapman R, Göd R, Niedermayr G, Wise MA (1989) Exsolution intergrowths of titanian ferrocolumbite and niobian rutile from the Weinebene spodumene pegmatites, Carinthia, Austria. Mineral Petrol 40:197–206

Claesson S, Williams IS (1987) Isotopic evidence for the Precambrian provenance and Caledonian metamorphism of high grade paragneisses from the Seve Nappes, Scandinavian Caledonides: I. conventional U–Pb zircon and Sm–Nd whole rock data. Contrib Mineral Petrol 97:196–204

Compston W, Williams IS, Meyer C (1984) U-Pb geochronology of zircons from lunar breccia 73217 using a sensitive high mass-resolution ion microprobe. J Geophys Res 89: B525–B534

Corfu F (2000) Extraction of Pb with artificially too-old ages during stepwise dissolution experiments on Archean zircon. Lithos 53:279–291

Dahl PS and Frei R (1995) Step-leach Pb-Pb dating of inclusion-bearing garnet and staurolite, with implications for Early Proterozoic tectonism in the Black Hills collisional orogen, South Dakota, United States. Geology 26:111–114

Davis DW, Krogh TE (2000) Preferential dissolution of ^{234}U and radiogenic Pb from alpha-recoil-damaged lattice sites in zircon; implications for thermal histories and Pb isotopic fractionation in the near surface environment. Chem Geol 172:41–58

Frei R, Biino GG, Prospert C (1995) Dating a Variscan pressure-temperature loop with staurolite. Geology 23:1095–1098

Frei R, Villa IM, Nägler ThF, Kramers JD, Przybylowicz WJ, Prozesky VM, Hofmann BA, Kamber BS (1997) Single mineral dating by the Pb-Pb step-leaching method: assessing the mechanism. Geochim Cosmochim Acta 61:393–414

Geisler T, Ulonska M, Schleicher H, Pidgeon RT, van Bronswijk W (2001) Leaching and differential recrystallization of metamict zircon under experimental hydrothermal conditions. Contrib Mineral Petrol 141:53–65

Geisler T (2002) Isothermal annealing of partially metamict zircon: evidence for a three-stage recovery process. Phys Chem Minerals 29:420–429

Goetze J, Kempe U, Habermann D, Nasdala L, Neuser RD, Richter DK (1999) High resolution cathodoluminescence combined with SHRIMP ion probe measurements of detrital zircons. Mineral Mag 63:179–187

Hanchar JM, Miller CF (1993) Zircon zonation patterns as revealed by cathodoluminescence and backscattered electron images: implications for interpretation of complex crustal histories. Chem Geol 110:1–13

Krogh TE (1973) A low-contamination method for hydrothermal decomposition method of zircon and extraction of U and Pb for isotopic age determination. Geochim Cosmochim Acta 37:485–494

Krogh TE (1982a) Improved accuracy of U-Pb zircon dating by selection of more concordant fractions using a high gradient magnetic separation technique. Geochim Cosmochim Acta 46:631–635

Krogh TE (1982b) Improved accuracy of U-Pb zircon ages by the creation of more concordant systems using an air abrasion technique. Geochim Cosmochim Acta 46:637–649

Kurz S (2000) Hydrothermale Alterationsprozesse in Zirkonen — Isotopengeologische und geochemische Implikationen. PhD Thesis, Univ Göttingen, 112 pp

Mattinson JM (1994) A study of complex discordance in zircons using step-wise dissolution techniques. Contrib Mineral Petrol 116:117–129

Mattinson JM (1997) Analysis of zircon by multi-step partial dissolution: the good, the bad, and the ugly. Geol Assoc Can Meet, Ottawa'97, Abstract A98

Mattinson JM (2000) U-Pb zircon analysis by "chemical abrasion": combined high-temperature-annealing and partial dissolution analysis. EOS Trans Am Geophys Union 81:S27

Mattinson JM (2001) Zircon radiation damage, annealing, dissolution, and Pb diffusion. 11th Annual VM Goldschmidt Conf, Abstr vol, 3625.pdf

Mattinson JM, Gaubard CM, Parkinson DL, McLelland WC (1996) U-Pb reverse discordance in zircons: the role of fine-scale oscillatory zoning and sub-microscopic transport of Pb. Am Geophys Union Geophys Monogr 95:355–370

McClelland WC, Mattinson JM (1996) Resolving high precision U-Pb ages from Tertiary plutons with complex zircon systematics. Geochim Cosmochim Acta 60:3955–3965

Meldrum A, Boatner LA, Weber WJ, Ewing RC (1998) Radiation damage in zircon and monazite. Geochim Cosmochim Acta 62:2509–2520

Murakami T, Chakoumakos BC, Ewing RC, Lumpkin GR, Weber WJ (1991) Alpha-decay event damage in zircon. Am Mineral 76:1510–1532

Nasdala L, Wenzel M, Vavra G, Irmer G, Wenzel T, Kober B (2001) Metamictisation of natural zircon: accumulation versus thermal annealing of radioactivity-induced damage. Contrib Mineral Petrol 141:125–144

Parrish RR (1987) An improved micro-capsule for zircon dissolution in U–Pb geochronology. Chem Geol 66:99–102

Petit J-C, Dran J-C, Paccanella A, Della Mea G (1989) Structural dependence of crystalline silicate hydration during aqueous dissolution. Earth Planet Sci Lett 93:292–298

Romer RL, Smeds S-A (1994) Implications of U-Pb ages of columbite-tantalites from granitic pegmatites for the Palaeoproterozoic accretion of 1.90–1.85 Ga magmatic arcs to the Baltic Shield. Precambrian Res 67:141–158

Romer RL, Smeds S-A (1996) U–Pb columbite ages of pegmatites from Sveconorwegian terranes in southwestern Sweden. Precambrian Res 76:15–30

Romer RL, Smeds S-A (1997) U–Pb columbite chronology of post-kinematic Palaeoproterozoic pegmatites in Sweden. Precambrian Res 82:85–99

Romer RL, Wright JE (1992) U–Pb dating of columbite: a geochronologic tool to date magmatism and ore deposits. Geochim Cosmochim Acta 56:2137–2142

Romer RL, Smeds S-A, Cerny P (1996) Crystal-chemical and genetic controls of U–Pb systematics of columbite-tantalite. Mineral Petrol 57:243–260

Sergeev SA, Meier M, Steiger RH (1995) Improving the resolution of single-grain U/Pb dating by use of zircon extracted from feldspar; application to the Variscan magmatic cycle in the Central Alps. Earth Planet Sci Lett 134:37–51

Sergeev SA, Komarov AN, Bickel RA, Steiger RH (1997) A new microtome for cutting hard submilimeter-sized crystalline objects for promoting high-resolution instrumental microanalysis. Eur J Mineral 9:449–456

Smith S (2001) Geochemistry and geochronology of rare-element pegmatites from the Superior province of Canada. PhD Thesis, The Open University, Milton Keynes, UK

Steiger RH, Bickel RA, Meier M (1993) Conventional U-Pb dating of single fragments of zircon for petrogenetic studies of Phanerozoic granitoids. Earth Planet Sci Lett 115:197–209

Tagami T, Carter A, Hurford AJ (1996) Natural long-term annealing of the zircon fission-track system in Vienna basin deep borehole samples: constraints upon the partial annealing zone and closure temperature. Chem Geol 130:147–157

Tilton GR (1960) Volume diffusion as a mechanism for discordant lead ages. J Geophys Res 65:178–190

Todt WA, Büsch W (1981) U–Pb investigations on zircons from pre-Variscan gneisses, I. A study from the Schwarzwald, West Germany. Geochim Cosmochim Acta 45:1789–1801

Trachenko KO, Dove MT, Salje EKH (2001) Atomistic modeling of radiation damage in zircon. J Phys Condens Matter 13:947–952

Trindle AG, Breaks FW (1998) Oxide minerals of the Separation Rapids rare-element granitic pegmatite group, northwestern Ontario. Can Mineral 36:609–635

Trindle AG, Breaks FW, Webb PC (1998) Wodginite-group minerals from the Separation Rapids rare-element granitic pegmatite group, northwestern Ontario. Can Mineral 36:637–658

Uher P, Cerny P, Chapman R, Hatar J, Miko O (1998) Evolution of Nb,Ta-oxide minerals in the Prasiva granitic pegmatites, Slovakia. II. External hydrothermal Pb,Sb overprint. Can Mineral 36:535–545

Vavra G, Gebauer D, Schmid R (1996) Multiple zircon growth and recrystallization during polyphase Late carboniferous to Triassic metamorphism of the Ivrea Zone (Southern Alps): an ion microprobe (SHRIMP) study. Contrib Mineral Petrol 122:337–358

Vavra G, Schmid R, Gebauer D (1999) Internal morphology, habit and U–Th–Pb microanalysis of amphibolite-to-granulite facies zircons: geochronology of the Ivrea Zone (Southern Alps). Contrib Mineral Petrol 134:380–404

Wasserburg GJ (1963) Diffusion processes in lead-uranium systems. J Geophys Res 68:4823–4845

Weber WJ, Ewing RC, Wang L-M (1994) The radiation-induced crystalline-to-amorphous transition in zircon. J Mater Res 9:688–698

White NM, Parrish RR, Bickle MJ, Najman YMR, Burbank D, Maithani A (2001) Metamorphism and exhumation of the NW Himalaya constrained by U-Th-Pb analyses of detrital monazite grains from early foreland basin sediments. J Geol Soc Lond 158:625–635

Wiedenbeck M (1995) An example of reverse discordance during ion microprobe zircon dating: an artifact of enhanced ion yields from a radiogenic labile Pb. Chem Geol 160:201–224

Ziegler JF, Biersack JP, Littmark U (1985) The stopping and range of ions in solids. In: Ziegler JF (ed) The stopping and range of ions in matter, vol 1. Pergamon, Oxford